AVERAGING BIAS CORRECTION FOR FUTURE IPDA LIDAR MISSION MERLIN

Yoann Tellier[1]*, Clémence Pierangelo[2], Martin Wirth[3], Fabien Gibert[1]

[1]*Centre National de Recherche Scientifique - Laboratoire de Météorologie Dynamique (CNRS - LMD), France, *yoann.tellier@lmd.polytechnique.fr*
[2]*Centre National d'Etudes Spatiales (CNES), France*
[3]*Deutsches Zentrum für Luft- und Raumfahrt (DLR), Germany*

ABSTRACT

The CNES/DLR MERLIN satellite mission aims at measuring methane dry-air mixing ratio column (XCH_4) and thus improving surface flux estimates. In order to get a 1% precision on XCH_4 measurements, MERLIN signal processing assumes an averaging of data over 50 km. The induced biases due to the non-linear IPDA lidar equation are not compliant with accuracy requirements. This paper analyzes averaging biases issues and suggests correction algorithms tested on realistic simulated scenes.

1 INTRODUCTION

Methane is the second most important anthropogenic greenhouse gas after carbon dioxide **Error! Reference source not found.**. A precise and accurate measurement of atmospheric CH_4 concentration on a global scale is crucial in order to improve the surface flux estimate and thus develop the knowledge of the global methane cycle [2].

The French-German spatial mission MERLIN (Methane Remote Sensing Lidar Mission) aims at measuring the methane dry-air mixing ratio (XCH_4) reaching unprecedented accuracy with targeted systematic error that is less than 0.2% relative error for all latitudes and all seasons.

Integrated Path Differential Absorption (IPDA) lidar measures the laser light (here short pulses) scattered back from the surface in order to retrieve the column content of a specific trace gas along the line of sight. Differential absorption uses the difference in transmission between the on-line signal with a wavelength set about the center of the CH_4 absorption line and the off-line signal which wavelength is significantly less absorbed. From these two signals the Differential Absorption Optical Depth (DAOD) of CH_4 is computed and the corresponding XCH_4 can be derived. The IPDA lidar equation (eq. (1) and (2)) links the backscattered off-line and on-line measurements to the sounded column of XCH_4 [3].

In order to reach the targeted 1% relative random error on XCH_4 measurements, the signal processing of MERLIN requires an horizontal averaging of data over 50 km along track. However, the non linearity of the IPDA lidar equation in combination with the variability of the observed scene (surface elevation, reflectivity, meteorology) along the averaging window induces a bias on the averaged data.

The present paper analyses and compares the biases of several averaging schemes and suggests correction algorithms. A comparative evaluation of the averaging schemes on realistic scenes is a key element to select the best approach (i.e. the least biased) for MERLIN processing.

2 METHODOLOGY

2.1 Principle of IPDA lidar

For every pair of on-line and off-line shots, the DAOD δ can be computed as [4]:

$$\delta = \frac{1}{2} \cdot \ln\left(\frac{P^{\text{off}} \cdot E^{\text{on}}}{P^{\text{on}} \cdot E^{\text{off}}}\right) = \frac{1}{2} \cdot \ln\left(\frac{Q^{\text{off}}}{Q^{\text{on}}}\right) \qquad (1)$$

where the on and off backscattered signal energies $P^{\text{on/off}}$ are normalized by the ratio of transmitted pulse energies $E^{\text{on/off}}$ ($Q^{\text{on/off}}$ is the normalized signals). Then, we can derive the XCH_4 as:

$$X_{CH_4} = \frac{\delta}{\int_0^{P_{\text{surf}}} WF(p,T) \cdot \mathrm{d}p} = \frac{\delta}{IWF} \qquad (2)$$

where P_{surf} is the pressure where the laser beam is backscattered and WF is the weighting function computed from external data describing the measurement sensitivity of XCH_4 along the line of sight.

These equations are valid for every shot-pairs but averaging over several successive shots is necessary to reach the targeted precision of the measurement.

2.2 Averaging strategies

For the following discussion we will use the triangular bracket notation to denote the arithmetic mean of the quantities Y_i associated to each pulse and the ΔY_i will represent the deviation to this arithmetic mean:

$$\langle Y \rangle = \frac{1}{N}\sum_{i=1}^{N} Y_i \quad \text{and} \quad \Delta Y_i = Y_i - \langle Y \rangle \tag{3}$$

There are four basic averaging schemes:

1. Averaging of XCH_4 (AVX):

$$\overline{X_{CH_4}}^{avx} = \langle \frac{\delta}{IWF} \rangle \tag{4}$$

2. Averaging of DAOD (AVD):

$$\overline{X_{CH_4}}^{avd} = \frac{\langle \delta \rangle}{\langle IWF \rangle} \tag{5}$$

3. Averaging of quotients (AVQ):

$$\overline{X_{CH_4}}^{avq} = \frac{\frac{1}{2} \cdot \ln \langle \frac{Q^{\text{off}}}{Q^{\text{on}}} \rangle}{\langle IWF \rangle} \tag{6}$$

4. Averaging of signals (AVS):

$$\overline{X_{CH_4}}^{avs} = \frac{\frac{1}{2} \cdot \left(\frac{\langle Q^{\text{off}} \rangle}{\langle Q^{\text{on}} \rangle} \right)}{\langle IWF \rangle} \tag{7}$$

As these equations are not linear and the physical quantities (surface pressure, surface reflectance...) vary for successive shot-pairs, the four averaging schemes are all biased in their own specific way. Correction algorithms must be applied in order to significantly reduce this averaging bias. AVQ (eq. (6)) has not been studied in this paper as the noise distribution leads to the highest bias.

2.3 Bias sources

Bias on DAOD from noise on $Q^{\text{on/off}}$:

As the measurements themselves are affected by noise it implies a bias when computing the XCH_4 for every averaging schemes. Indeed, we can write $Q^{\text{on/off}}$ as the sum of their noiseless mean signals $Q_{\text{true}}^{\text{on/off}}$ and a noise term $\Delta Q^{\text{on/off}}$. From this decomposition we can show that for any shot-pair i the true DAOD is biased:

$$\delta_i = \delta_{i,\text{true}} + \ln\left(1 + \frac{\Delta Q_i^{\text{off}}}{Q_{i,\text{true}}^{\text{off}}}\right) - \ln\left(1 + \frac{\Delta Q_i^{\text{on}}}{Q_{i,\text{true}}^{\text{on}}}\right) \tag{8}$$

In the case where the noise follows a normal distribution and has low amplitude (i.e. $\Delta Q_i^{\text{on/off}} / Q_{\text{true}}^{\text{on/off}} \ll 1$), the bias term can be approximated as:

$$\delta_i - \delta_{i,\text{true}} = \frac{1}{4}\left(\frac{1}{(SNR_i^{\text{on}})^2} - \frac{1}{(SNR_i^{\text{off}})^2}\right) \tag{9}$$

Where $SNR^{\text{on/off}}$ are the on-line and off-line signal to noise ratios. Providing high enough SNRs the bias produced by the measurement noise can be estimated.

Bias from shot-by-shot geophysical variations:

Variations of surface reflectivity impacts the AVS. Indeed, this scheme is more sensitive to targets with high reflectivity (i.e. high value of Q_i^{off}) as shown by the following equation:

$$\begin{aligned} \delta^{avs} &= -\frac{1}{2} \cdot \ln\left(\frac{\langle Q^{\text{on}} \rangle}{\langle Q^{\text{off}} \rangle}\right) \\ &= -\frac{1}{2} \cdot \ln\left(\sum_{i=1}^{N} \frac{Q_i^{\text{off}}}{N \cdot \langle Q^{\text{off}} \rangle} \cdot e^{-2 \cdot \delta_i}\right) \end{aligned} \tag{10}$$

This sum is the weighted average of the shot-by-shot transmissions weighted by the off-signal variations (i.e. proxy of reflectivity variations):

$$w_i = \frac{Q_i^{\text{off}}}{\sum_{k=1}^{N} Q_k^{\text{off}}} \tag{11}$$

So low reflectivity regions contribute less to the average.

Then, when there is a variation of geophysical quantities (e.g. topographic or surface pressure variations) there is a discrepancy between the average DAOD and the single-shot DAOD:

$$\Delta\delta_i = \delta_{i,\text{true}} - \langle \delta \rangle \tag{12}$$

We can derive the bias from equation (10) as:

$$\delta^{avs} - \langle \delta \rangle = -\frac{1}{2} \cdot \ln\left(\sum_{i=1}^{N} w_i \cdot e^{-2 \cdot \Delta\delta_i}\right) \tag{13}$$

Bias when averaging concentrations:

Directly averaging XCH_4 (eq. (4)) is not equivalent to averaging DAOD and IWF separately (eq. (5)). In the first case, we average concentrations and not molecules. So, there is the same contribution from columns with many molecules as from ones with less molecules.

The difference between the two approaches is described by:

$$\overline{X_{CH_4}}^{avd} - \overline{X_{CH_4}}^{avx} = \frac{1}{N}\sum_{i=1}^{N} \frac{\Delta IWF_i}{\langle IWF \rangle} \cdot X_{CH_4,i} \qquad (14)$$

As presented above, several sources of bias appear when computing the average mixing ratio of CH_4. The following section exposes the algorithms that correct for those biases in a practical way.

2.4 Correction algorithms

- For AVX, we need to correct the following sources of bias: bias induced by noise on $Q^{\mathrm{on/off}}$ (eq. (9)) and averaging of concentration instead of molecules (eq. (14)).

- For AVD and averaging of IWF, we only need to correct the bias induced by the noise on $Q^{\mathrm{on/off}}$ (eq. (9)).

- For AVS and averaging of IWF, several corrections need to be implemented. As AVS is more sensitive to the high reflectance area, the averaging of IWF must be done with consistent weights (eq. (11)):

$$\langle IWF \rangle_w = \sum_{i=0}^{N} w_i \cdot IWF_i \qquad (15)$$

Furthermore the DAOD from averaging signals is biased according to equation (13). It is possible to evaluate this bias by considering as a first order approximation the DAOD computed from average signals pondered by the relative fluctuations of IWF:

$$\Delta\delta_i \approx \delta^{avs} \cdot \frac{\Delta IWF_i}{\langle IWF \rangle_w} \qquad (16)$$

This process could be turned into an iterative correction (beyond the scope of this paper).

Then the last correction to take into account is the bias induced by the equivalent noise on the averaged signals. The resulting SNR can be computed by averaging signals and taking the quadratic mean of the standard deviations in order to apply equation (9).

2.5 Simulation description

The aim of the simulation is to estimate the biases of estimated XCH_4. A global description of the simulation is presented on Figure 1.

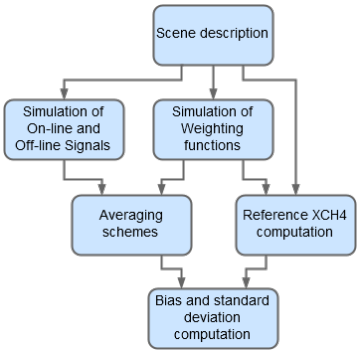

Figure 1 Global description of the simulation

Each simulation considers a typical number of 150 pulses per averaging window, approximately corresponding to 50km. It relies on a description of the CH_4 field, surface pressure and reflectivity description. Then, on-line and off-line signals are computed from surface reflectivity and noise simulation. The weighting functions for each pulse are computed using CH_4 absorption cross-sections from the 4A radiative transfer model [5] and are integrated vertically. Next, we proceed to the computation of averaged XCH_4 on 50km with the different schemes described in section 2.2 and the correction algorithms described in section 2.4.

The number of random samples for noise simulation has to be considerable in order to compute the biases with sufficient accuracy. The simulation described above is repeated 300.000 times to reach an accuracy on the bias of approximately 0.1 ppb for the nominal case (reflectivity of 0.1). This simulation has been tested on realistic scenes.

2.6 Realistic scenes

The averaging schemes have been tested on three realistic scenes located in France (Toulouse, Millau and Chamonix). The physical data and their sources are: Reflectivity from SPOT5, SRTM topography and Interpolated surface pressure from ECMWF.

The scenes have been chosen to be representative of the main geophysical variations that can produce bias on XCH_4 estimation. Toulouse, Millau and Chamonix respectively present medium, high and extreme altitude variations (cf. Figure 2) and the same trend for reflectivity variations. The mean reflectivity can be tuned.

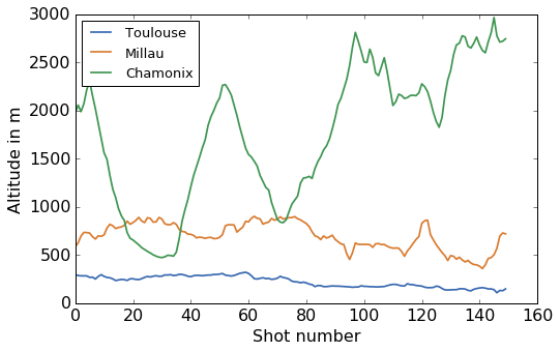

Figure 2 Altitude for the 3 studied scenes

3 RESULTS

The results of the simulation are shown in Figure 3. The averaging scheme that is globally the least biased is AVS. For all reflectivity, the bias stays limited to less than 0.7 ppb. The main cause of bias for this scheme is topographic or meteorological variation.

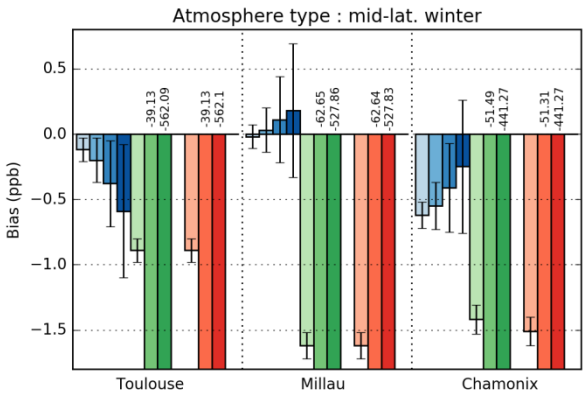

Figure 3 Residual Biases on a 50 km window for the three scenes (Toulouse, Millau, Chamonix) - for the three averaging schemes (blue shades for AVS, green shades for AVD and red shades for AVX) - for four different mean reflectivity (from light to dark colors decreasing reflectivity - 0.1 vegetation ; 0.05 mixed water/vegetation ; 0.025 sea/ocean ; 0.016 ice/snow) - The biases are displayed over the bars that end outside the frame.

AVD and AVX schemes are more affected by the ground reflectivity. The correction given by equation (9) is efficient when reflectivity is high. However, for a lower reflectivity the correction is no longer valid because it comes from a Taylor expansion assuming low amplitude of the noise.

4 CONCLUSIONS

This study shows that it is possible to limit the bias induced by the averaging scheme when an appropriate bias correction is implemented. The AVS scheme is less biased than other schemes in all simulated cases and below the target of 1 ppb allocated for this type of error. An alternative solution would be to take advantage of the two schemes: averaging signals on smaller windows where there is less geophysical variation until we reach a higher SNR that is compliant with the approximation of SNR correction (eq. (9)). Then averaging the resulting columns together on the 50 km window. Current development of this study tends to show that this combined scheme is not better than AVS results. Further studies will check the impact of an imprecise estimation of SNR on the bias correction (eq. (9)).

ACKNOWLEDGEMENTS

The authors wish to express special thanks to Fabien Marnas (Capgemini Technology Services for CNES) for the provision of the interpolated meteorological data used in this study.

References

[1] IPCC, 2013: *Climate Change 2013: The Physical Science Basis. Contribution of Working Group I to the Fifth Assessment Report of the Intergovernmental Panel on Climate Change*. Cambridge University Press, Cambridge, United Kingdom and New York, NY, USA, 1535 pp.

[2] P. Bousquet et al.: Contribution of anthropogenic and natural sources to atmospheric methane variability. Nature 443, 439-443 Available from: 10.1038/nature05132

[3] M. Bode et al., 2014: MERLIN: an integrated path differential absorption (IPDA) lidar for global methane remote sensing, *Proc. of ICSO* 2014, Tenerife, Canary Islands.

[4] C. Pierangelo et al., 2016: MERLIN (methane remote sensing lidar mission): an overview, *Proc. of 27th ILRC*, New York City, USA.

[5] Scott N.A. et al., 1981: A fast line-by-line method for atmospheric absorption computations: The Automatized Atmospheric Absorption Atlas. J. Appl. Meteor., 20,802-812.